

Structural Organization of (Na⁺ + K⁺)-ATPase in Purified Membranes

G. ZAMPIGHI, J. KYTE,* and W. FREYTAG[†]

Department of Anatomy and Jerry Lewis Neuromuscular Research Center, UCLA School of Medicine, Los Angeles, California 90024; *Department of Chemistry, D-006, University of California, San Diego, La Jolla, California 92093; [†]E. I. Du Pont de Nemours, Photo Products Department, Experimental Station, Wilmington, Delaware 19898

ABSTRACT The structural organization of crystalline, membrane-bound (Na⁺ + K⁺)-ATPase was studied by negative staining and thin sectioning. The enzyme molecules were induced to form crystalline arrays within fragments of membrane by incubation in defined ionic conditions. The enzyme remained fully active after crystallization. Negative staining and computer processing of images of the crystalline specimens identified two discrete crystalline arrays. The dimensions of the unit cell of one of the arrays were large enough to accommodate an $\alpha\beta$ protomer; those of the other array, an $(\alpha\beta)_2$ diprotomer. Thin sections of the crystalline fraction contained a unique membrane complex that was formed from two apposed plasma membranes. The paired membranes in this complex were separated by a center-to-center space of 15 nm containing evenly spaced septa that connected the membrane surfaces; the overall thickness of the entire structure was 22–25 nm. The agglutinin from *Ricinus communis*, a lectin that binds to the carbohydrate moiety of the β -subunit of (Na⁺ + K⁺)-ATPase, decorated the free surfaces of the complex. Therefore, this complex of paired membranes is the result of interactions between the cytoplasmic domains of the enzyme. From measurements of the dimensions of these structures, we estimate the overall length of the enzyme to be ~11.5 nm along the axis perpendicular to the plane of the membrane, and the molecular protrudes more (~5 nm) on the cytoplasmic surface than on the extracytoplasmic surface (~2 nm).

Sodium and potassium ion-activated adenosine triphosphatase [(Na⁺ + K⁺)-ATPase]¹ is inserted into the plasma membranes of animal cells where it generates and maintains the high potassium and low sodium concentrations in the cytoplasm. The consequent differences in the steady-state concentrations of these cations between the cytoplasm and the extracellular environment provide the potential energy to maintain cellular volume, to drive the uptake of nutrients, to move water across epithelia, and to create the resting potentials of cells.

(Na⁺ + K⁺)-ATPase has been isolated from, among other sources, mammalian kidney (20, 21), elasmobranch rectal gland (18), and piscine electric organ (8). All of the enzymes purified so far are composed of two kinds of subunits: one is

a large, relatively hydrophobic protein, and the other is a smaller, sialoglycoprotein (22). The minimum asymmetric unit of the mammalian renal enzyme, the $\alpha\beta$ protomer,² is formed from one large polypeptide (α , molecular weight = 110,000 ± 10,000) and one small polypeptide (β , molecular weight = 50,000 ± 5,000), which together form a complex whose total molecular weight is 160,000 ± 15,000 (4, 22, 26, 32). This number is consistent with a value, obtained in recent titrations of purified enzyme, of one active site (175,000 ± 10,000 daltons of proteins)⁻¹ (28). Although the α and β

² The following terminology will be used to define the polypeptide composition of a given molecular complex. The unit composed of one α polypeptide and one β polypeptide will be termed the $\alpha\beta$ protomer; the unit composed of two α polypeptides and two β polypeptides, the $(\alpha\beta)_2$ diprotomer; and so forth. A lattice formed from unit cells, each containing an $\alpha\beta$ protomer, will be designated protomeric; one formed from unit cells, each containing an $(\alpha\beta)_2$ diprotomer, diprotomeric.

¹ Abbreviations used in this paper: (Na⁺ + K⁺)-ATPase, sodium and potassium ion-activated adenosine triphosphatase; TES, 2-[[Tris-(hydroxymethyl) methyl]-amino] ethanesulfonic acid.

polypeptides together form the minimum asymmetric unit of the enzyme, the active site (39), the site to which cardiac glycosides bind (34), and the sulfhydryl residue whose modification inactivates the enzyme (43) are all located on the α polypeptide.

Recent studies of $(\text{Na}^+ + \text{K}^+)\text{-ATPase}$ have focused on the determination of the minimum unit necessary for enzymatic function (25). One approach to this issue has been to dissolve membranes with nonionic detergents under conditions favoring the dissociation of discrete protein complexes from each other (3, 6, 11, 14). However, there has been some disagreement concerning the hydrodynamic properties of the complexes formed in this process (3, 11, 14). Recently, Craig (5) has used the technique of stoichiometric intramolecular cross-linking (5, 17) to show that different complexes are present in these solutions. Also, he has been able to prepare a monodisperse solution of the protomer dissolved in a solution of the nonionic detergent, octaethyleneglycol dodecyl ether (6). This discrete protomer is the smallest unit yet prepared that can display enzymatic activity. This has eliminated theories that were based on the hypothesis that the $(\alpha\beta)_2$ dimer was required for function (24).

Another approach to the issue of the minimum function unit of the enzyme has involved determinations of the ultrastructural organization of the enzyme in its membrane-bound form. In previous investigations (7, 13, 40, 41), the $(\text{Na}^+ + \text{K}^+)\text{-ATPase}$ has been characterized by negative staining and freeze-fracture electron microscopy. Recently, crystalline arrays of membrane-bound $(\text{Na}^+ + \text{K}^+)\text{-ATPase}$ have been prepared by prolonged incubation with either phosphate or magnesium and vanadate (16, 38). Projection maps calculated from micrographs of these crystalline arrays, showed that those induced by vanadate contained only protomer in the unit cell, while those induced by phosphate contained $(\alpha\beta)_2$ dimer. This report will describe the overall shape, sizes, and dimensions of the different domains of $(\text{Na}^+ + \text{K}^+)\text{-ATPase}$ molecules within crystalline lattices. We have found that each $\alpha\beta$ protomer is a prolate ellipsoid ~ 12 nm long that is asymmetrically situated in the lipid bilayer. It protrudes more (~ 5 nm) on the cytoplasmic surface than on the extracytoplasmic surface (~ 2 nm). A preliminary report of some of these observations has been presented (44).

MATERIALS AND METHODS

SDS was purchased from Sigma Chemical Co. (St. Louis, MO) and further purified by crystallization from 90% ethanol. Imidazole was recrystallized from benzene and then acetone. The agglutinin from *Ricinus communis* was kindly provided by Dr. Nathan Kaplan, University of California at San Diego. The agglutinin readily agglutinates human erythrocytes and PAGE (42) of it showed only two subunits, $M_r = 30,000$ and $M_r = 35,000$ (31).

$(\text{Na}^+ + \text{K}^+)\text{-ATPase}$: The starting material for all of the preparations of $(\text{Na}^+ + \text{K}^+)\text{-ATPase}$ examined in these studies was microsomes prepared from the medullas of canine kidneys by the method of Jørgensen and Skou (19) as modified by Kyte (21). The microsomal fractions were submitted to titrations with either sodium deoxycholate (12, 21) or SDS (20).

The procedure of Jørgensen (20) was explored to determine the effect of changing the ratio of detergent to protein on the purity, size, and particle density of the microsomal membranes. A suspension containing 2.0 mg protein ml^{-1} microsomes, 3 mM Na_2ATP , 1 mM Na_2EDTA , and 25 mM imidazolium chloride, pH 7.5, was treated with concentrations of SDS that varied over the set of samples (0.0; 0.4; 0.5; 0.6; 0.65; 0.7 mg ml^{-1}). Each sample was centrifuged on discontinuous gradients of sucrose and the interface between 37.3% and 28.8% sucrose was collected from each gradient (29). Negative staining demonstrated that the microsomes exposed to 0.6 mg ml^{-1} SDS yielded the largest fragments of membrane with the highest density of particles (see Fig. 2D).

A sample was then prepared whose final concentrations were 2.0 mg ml^{-1}

microsomes, 3 mM Na_2ATP , 1 mM Na_2EDTA , 0.6 mg ml^{-1} SDS, 25 mM imidazolium chloride, pH 7.5. This sample was injected onto a gradient of sucrose between 10 and 45% formed in a Ti 14 zonal rotor (Beckman Instruments, Palo Alto, CA) such that the concentration of sucrose was a linear function of the rotor's radius. After 150 min at 45,000 rpm, sufficient to bring the membranes to their equilibrium density (20), the gradient was collected. 9–12 fractions contained $(\text{Na}^+ + \text{K}^+)\text{-ATPase}$ activity, and they were collected separately and systematically examined by negative staining. The largest membranes with the highest density of particles were found in the two or three fractions just to the denser side of the center of the peak of activity (see Fig. 12D). The membranes were washed by centrifugation and resuspended at 2–3 mg protein ml^{-1} in 0.25 M sucrose, 1 mM Na_2EDTA , 0.1% 2-mercaptoethanol, and 30 mM histidinium chloride, pH 7.1. The membrane suspension was divided into aliquots of 50 μl liters, frozen in liquid nitrogen, and stored at -70°C .

Crystallization: Two-dimensional crystals of isolated, membrane-bound $(\text{Na}^+ + \text{K}^+)\text{-ATPase}$ were produced by systematically altering the ionic compositions of the medium. A typical experiment was performed by diluting 20 μl liters of a suspension of membranes (2–3 mg protein ml^{-1} in storage solution) with 150 μl liters of the solution in which production of the arrays was to be tested. The resulting mixture was centrifuged in a Beckman airfuge (Beckman Instruments) for 60 min at 100,000 g. The pellet was resuspended in 100 μl liters of the same solution, and the formation of two-dimensional arrays was monitored by negative staining.

We found that the conditions necessary to produce crystals rapidly, over < 1 h, were the presence of a divalent metal ion and inorganic phosphate or orthovanadate and the absence of Na^+ . The replacement of K^+ with NH_4^+ or Tris was not necessary to produce crystals, but the specimens consistently showing extensive crystallization usually contained NH_4^+ . We discovered the best composition for the mixture by varying the concentrations of the necessary ingredients and observing the crystallinity and reproducibility of the arrays. We varied the concentration of Mg^{2+} from 5 to 120 mM, Mn^{2+} from 1 to 5 mM, inorganic phosphate from 1 to 5 mM, and orthovanadate from 20 to 400 μM . The best ionic combination was a solution containing 10 mM MgCl_2 , 1 mM MnCl_2 , 5 mM H_3PO_4 , 25 mM 2-[(Tris - (hydroxymethyl) methyl]-amino) ethane sulfonic acid (TES), adjusted to pH 6.8 with NH_4OH . The substitution of orthovanadate for inorganic phosphate did not substantially improve the size or coherence of the crystalline patches.

Negative Staining and Image Processing: Aliquots of crystalline and noncrystalline $(\text{Na}^+ + \text{K}^+)\text{-ATPase}$ were deposited on freshly prepared carbon-coated grids and washed with 1–2% uranyl acetate. The grids were scanned at low magnification to select those areas having membranes surrounded by thin films of stain. The membranes were photographed at $\times 40,000$ magnification, at minimum exposure with a microfocusing device (Zeiss, Oberkochen, Federal Republic of Germany). They were recorded sufficiently close to focus that the contrast transfer function was uniform over the spacing of interest (9). All the microscopy was performed in either a Zeiss EM10C or EM109 electron microscope at acceleration voltages of 80–100 kV.

The negatives were studied by inspecting their optical transforms in an optical diffractometer constructed according to the model described by Salmon and DeRosier (35). The areas within the negatives that were chosen for analysis by computer methods (for a review see reference 2). They were selected on the basis of the symmetry and the extent of the resolution observed in the optical diffraction patterns. The selected areas were then scanned at 25- μm intervals with an automatic microdensitometer to produce arrays of digitized densities. These arrays were Fourier transformed in an IBM 3033 or VAC 11/780 computer. Peak amplitudes and phases were collected from these transforms for each lattice reflection. The phases of all the projections were refined to a common origin, and computer-filtered maps were calculated by carrying out inverse Fourier transformation.

Thin Sectioning: Membrane-bound $(\text{Na}^+ + \text{K}^+)\text{-ATPase}$, bathed in storage solution, was diluted with 3% glutaraldehyde in 0.2 M sodium cacodylate, pH 7.4. After 1 h at 4°C , the suspension of membranes was pelleted by centrifugation. Pellets of membranes containing crystalline $(\text{Na}^+ + \text{K}^+)\text{-ATPase}$ were fixed for 30 min with 3% glutaraldehyde in crystallizing solution, followed by an additional 90 min of fixation with 3% glutaraldehyde in 0.2 M sodium cacodylate, pH 7.4. All of the pellets were postfixed in 2% osmium tetroxide in 0.1 M sodium cacodylate, dehydrated in ethanol, and embedded in Epon 812.

Decoration of Membranes with Agglutinin from *Ricinus communis*: Membrane-bound $(\text{Na}^+ + \text{K}^+)\text{-ATPase}$ (0.2–0.3 mg of protein) was diluted with 2 ml of crystallization medium. The suspension was centrifuged for 1 h at 30,000 rpm in a Beckman 40.3 rotor (Beckman Instruments). The resulting pellets were resuspended in 0.1 ml of crystallization medium, and then 0.2 ml of a 1 mg ml^{-1} solution of the agglutinin from *Ricinus communis* (31) was added to the suspension. The membranes were

collected by centrifugation, and the pellets were fixed in 0.3 ml of a solution containing 4% glutaraldehyde, 0.3% tannic acid, 0.1 M sodium cacodylate, pH 7.3 (36). After 1–2 h at 4°C, the solution was deposited on top of a piece of Millipore filter (Millipore Corp., Bedford, MA), type VSWP, with its shiny side up. The piece of filter and the suspension were supported on an adapter that had been cast from Epoxy resin and that fits into the bottom of a Beckman SW60 Ti rotor tube. The membranes were deposited on the surface of the filter by centrifugation at 20,000 rpm for 90 min. The filter was washed, postfixed in osmium tetroxide, and dehydrated in ethanol. The membranes and what remained of the filter were soaked in a mixture of equal parts of ethanol and Epon 812 for 1 h, and passed through propylene oxide/Epon 812 mixtures and embedded in pure Epon 812 (36).

Sections displaying a gray interference were cut with a diamond knife mounted on a MT-5000 Sorvall ultramicrotome (DuPont Co., Newton CT) and deposited on carbon-coated grids. The sections were triply stained on the grids with uranyl acetate, lead citrate, and bismuth subnitrate (33).

RESULTS

Preparation and Characterization of the Specimens

The formulation of crystalline specimens of membrane-bound ($\text{Na}^+ + \text{K}^+$)-ATPase was studied by systematic modifications of the ionic composition of the medium. Skriver et al. (38) have reported that the formation of such arrays required prolonged incubations of up to 4 wk with sodium vanadate in the presence of magnesium, a treatment leading to significant inactivation of the enzyme. We have extended these observations by studying the effect of varying the concentrations of Mg^{2+} , Mn^{2+} , inorganic phosphate, and orthovanadate. The medium that produced crystallization in the most reproducible fashion was 10 mM MgCl_2 , 1 mM MnCl_2 , 5 mM H_3PO_4 , 25 mM TES adjusted to pH 6.8–7.0 with NH_4OH . Replacing the inorganic phosphate with Na_3VO_4 in concentrations up to 400 μM did not improve the extend on crystallinity. The important conditions seem to be the absence of Na^+ , the presence of Mg^{2+} , and inorganic phosphate. The medium produced crystallization in most of the membranes present in a fraction of, at least, 30 separate experiments. This crystallization medium has the advantage that the incubation time necessary to produce the crystals has been shortened from several weeks (16, 38) to <2 h. Moreover, this procedure has the additional advantage over previous methods in that the crystallized membranes retained >95% of their original ($\text{Na}^+ + \text{K}^+$)-ATPase activity.

Various purification procedures for ($\text{Na}^+ + \text{K}^+$)-ATPase were explored to find conditions that produce large membrane fragments with dense particle populations (see Fig. 2D). We have analyzed specimens isolated from two different purification procedures (20, 22). In these specimens, we have studied the characteristics of the membranes gathered at several different buoyant densities and the effects of varying the concentrations of key solutes on the crystallization of the enzyme molecules. The protocol that produced the specimens used in this study is as follows: Microsomes suspended at 2.0 mg ml^{-1} protein in a solution of 0.6 mg ml^{-1} SDS were submitted to isopycnic centrifugation on a continuous gradient of sucrose. The membranes with a buoyant density of 1.13 ± 0.1 g ml^{-1} (20) were collected and used for our studies.

The membranes isolated through these slight modifications of the published procedure were studied by SDS gel electrophoresis to show that they contained ($\text{Na}^+ + \text{K}^+$)-ATPase at a level of purity high enough to preclude the possibility that the arrays produced arose from contaminants. A scan of a polyacrylamide gel of the isolated fraction is shown in Fig. 1A. The majority of the protein is accounted for by the α and

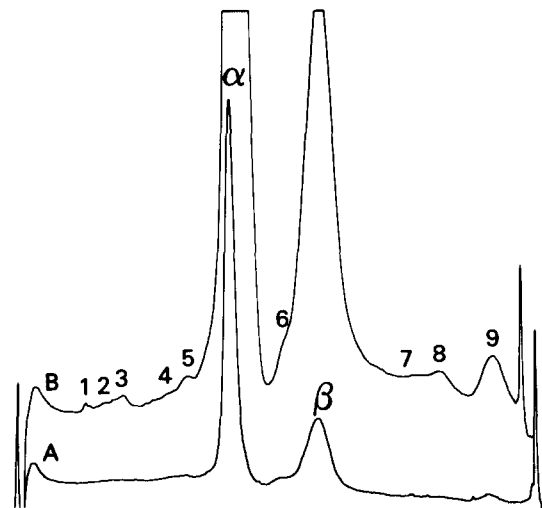
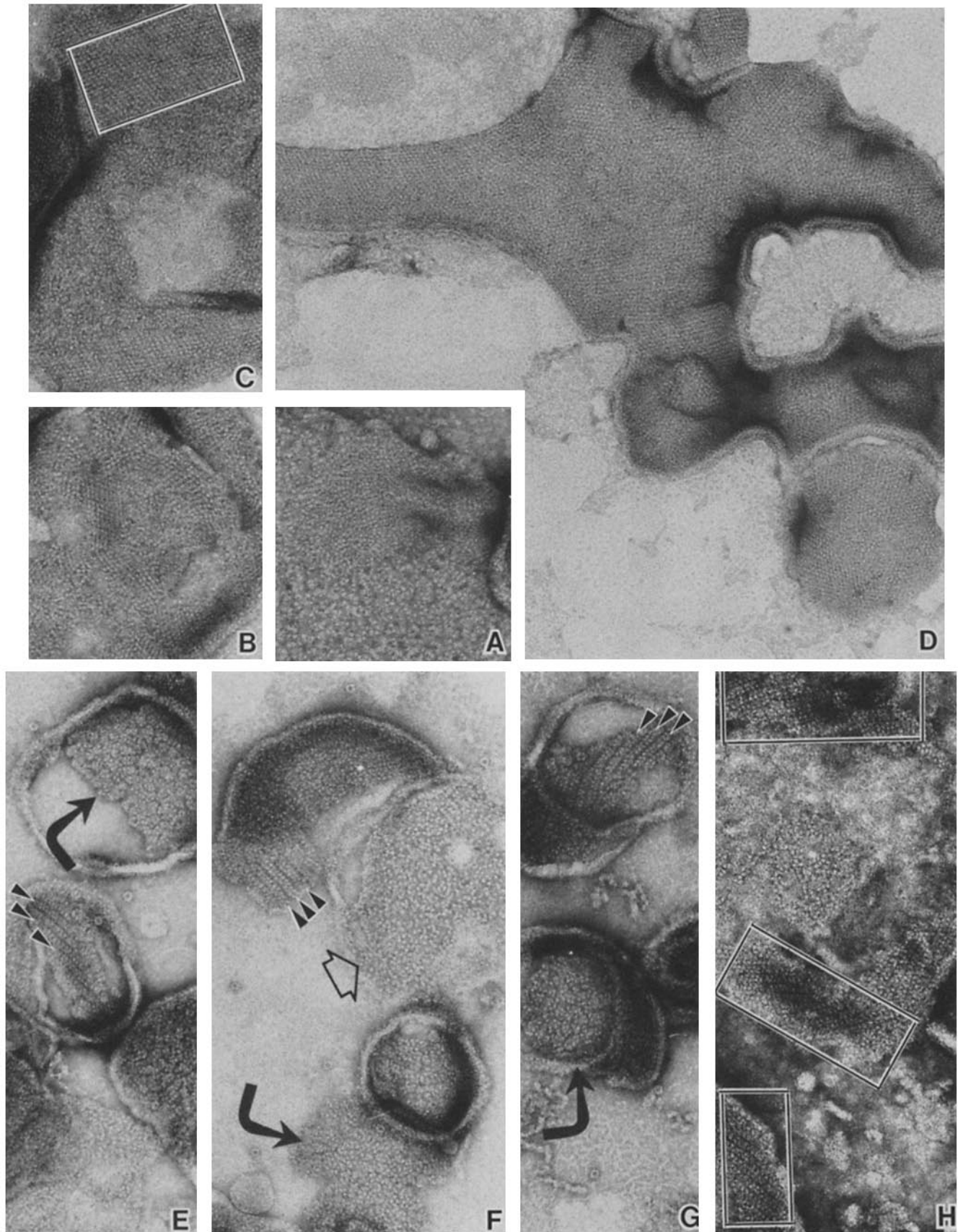


FIGURE 1 Scans of polyacrylamide gels loaded with 10 μl (A) and 75 μl (B), respectively, of the same sample of ($\text{Na}^+ + \text{K}^+$)-ATPase dissolved in a solution of SDS. The membrane fragments in a suspension of purified ($\text{Na}^+ + \text{K}^+$)-ATPase were dissolved in a solution prepared so that the final concentrations would be 0.3 mg protein ml^{-1} , 1.5% 2-mercaptoethanol, 3% SDS, 0.2 M sucrose, 20 mM imidazolium chloride, pH 7.5. The solution was brought to 100°C for 1 min and samples were then added to gels of 5% polyacrylamide cast in 0.1% SDS according to the procedure of Weber and Osborn (42). Direction of electrophoresis is from left to right and the ordinate is absorbance at 630 nm. Scan A, from a lightly loaded gel, shows that the majority of the protein is accounted for by the α and β polypeptides of the enzyme. Scan B is from a heavily overloaded gel and impurities in the preparation (labeled from 1 to 9) could be readily detected.

β polypeptides of ($\text{Na}^+ + \text{K}^+$)-ATPase (22), but impurities (labeled 1–9) can be detected on the scan of a heavily overloaded gel (Fig. 1B). A sample of the enzyme (~ 100 μg of protein) was dissolved in a solution of SDS, and 5 μl , 10 μl , 15 μl , 20 μl , 25 μl , and 75 μl of this mixture were loaded on successive gels. Scans of all of these gels were made, and the areas of absorbance corresponding to all components on every gel were calculated. The areas of absorbance of the α and β polypeptides were linear functions of the volume added to the gel up to 25 μl . The areas of the impurities (components 1–9) were determined from the scan of the gel containing the 75 μl of sample (Fig. 1B). These areas and the slopes of the plots of areas of absorbance of the α and β polypeptides against volume were used to calculate the percentage of the total protein constituted by each impurity. In two separate preparations of the enzyme, examined on several overloaded gels, impurities labeled 1–9 averaged 0.2%, 0.3%, 0.4%, 0.4%, 0.4%, 1.3%, 1.9%, 2.6%, and 2.5%, respectively, of the total protein. The specific enzymatic activity (23) of these preparations was 800 $\mu\text{mol mg}^{-1}\text{h}^{-1}$.

If it is assumed that all of the organic phosphate (1) present in these preparations is from phospholipid, then there are 180 mol of phospholipid ($\text{mol of } \alpha\beta^{-1}$). These membranes contain also about 120 mol of cholesterol ($\text{mol of } \alpha\beta^{-1}$) (20), which, together with the phospholipid, should give an area³ of 140–150 nm^2 of bilayer ($\alpha\beta^{-1}$) (25).

³ The surface area of bilayer was obtained from reference 26. The area per molecule of a 3:2 lecithin/cholesterol mixture is ~ 0.48 nm^2 . Because there are ~ 300 mol of lipid per $\alpha\beta$ it follows that there are ~ 140 –150 nm^2 of bilayer per mole of $\alpha\beta$ -protomer.



Negative Staining

The noncrystalline specimens produced views very similar to those published previously by others (7, 13, 40, 41). They contained fragments of membranes of different sizes and shapes whose surfaces were covered with particles of 4–5-nm diam.

When the membrane fragments were suspended in crystallization medium, the particles changed their organization in the plane of the membrane (Fig. 2). On the same grid, containing specimens all exposed to the same solutions, several arrangements could be observed. The membrane indicated by the wide arrow in Fig. 2*F*, displays well-defined, randomly distributed particles. The membrane fragments indicated by the curved arrows in Fig. 2, *E*, *F*, and *G* show particles that have associated by forming small circular clusters comprised of four to six individuals. Another type of particle association is presented in Fig. 2*A* where a region of the membrane is covered by a large, tightly packed but disorganized cluster of particles. Also present are regular arrays that were either partially or completely formed examples of two distinct crystals. We shall refer to these two distinct crystalline arrangements of membrane-bound ($\text{Na}^+ + \text{K}^+$)-ATPase molecules as protomeric and diprotomeric.²

Examples of the protomeric array are shown in Fig. 2, *B* and *C*. The fragments of membrane shown in these micrographs are composed almost entirely of single membranes, and the particles are aligned in rows that intersect at oblique angles. The distances between the rows are ~ 6 nm in one direction and ~ 5 nm in the other and the included angle between these rows is 66° . Paired membranes recognizable by their thicker edge, also displayed protomeric arrays having similar spacings (Fig. 2*D*).

Selected views of diprotomeric arrays of molecules of ($\text{Na}^+ + \text{K}^+$)-ATPase are presented in Fig. 2, *E*, *F*, and *G* and enclosed in rectangles in Fig. 2*H*. This lattice is characterized by ribbons that are composed of two parallel rows of particles. Each ribbon is 9–10 nm wide and repeats at ~ 12.5 nm center-to-center.

Optical Diffraction and Image Processing

Optical diffraction was used to screen a large number of images. This was done to determine their most reproducible features and to select the images for processing by a computer. The best images were considered to be those whose diffraction patterns had the largest number of spots and extended to the highest resolution and in which these diffraction spots stood out clearly from the noise of the background (10). For example, one of the optical diffraction patterns obtained from the protomeric array had five diffraction spots, which are indexed in Fig. 3*B*. The (1,0) reflection, normally the strong-

est, is located at a distance of $1/6.2 \text{ nm}^{-1} (\pm 0.36)$, whereas the (0,1) reflection extends to $1/4.8 \text{ nm}^{-1} (\pm 0.57)$ from the origin. The spot indexed as (2,1), $\sim 1/2.7 \text{ nm}^{-1}$, was present in just a few images and represents the highest resolution we have accomplished in this type of crystal. The *a/b* ratio of the two skew lattice vectors varied from 1.2 to 1.4, and their included angle varied from 64° to 70° .

Several crystals of the protomeric array were also studied by processing the images by Fourier methods (2). The resulting projection maps (Fig. 3*C*) display the parts of the ($\text{Na}^+ + \text{K}^+$)-ATPase that exclude negative stain. The map shows that each asymmetric unit has an elliptical shape. A consistent feature of all the maps calculated thus far was a small elongation of one pole of the ellipse. These maps are similar to those presented by Herbert et al. (16) for the crystals formed during incubation in 0.25 mM sodium monovanadate.

The optical diffraction patterns of diprotomeric crystals (Fig. 4*B*) presented several characteristic features. The (1,0) reflection was located at $\sim 1/12.5 \text{ nm}^{-1}$, whereas the (0,1) reflection extended to $\sim 1/5.5 \text{ nm}^{-1}$, and the included angle of the unit cell was $72\text{--}80^\circ$. A projection map calculated from these crystals is shown in Fig. 4*C*. The maps show that each unit cell contains two somewhat elliptical peaks. In the particular map displayed, the two adjacent peaks are different in the sense that one is rounder and larger and the other more elliptical and smaller. These differences could arise, however, from uneven staining of these crystals. The maps obtained from the diprotomeric crystal did not present asymmetric units subdivided into two peaks such as those described by Herbert et al. (16) for the crystals prepared by incubation of the enzyme in 12.5 mM phosphate.

Thin Sectioning

Pellets of the isolated, membrane-bound ($\text{Na}^+ + \text{K}^+$)-ATPase suspended in storage and crystallization media were examined by thin sectioning. Typical fields from one of these specimens are presented in Figs. 5 and 6. Fig. 5 shows membranes of variable size and shape, and closed vesicles or cupped structures 0.3–0.7 μm in diameter. No particular pattern of intermembrane associations was observed in these sections. The membranes that were first suspended in the crystallization medium and then examined by thin sectioning (Fig. 6), showed a new structure. This new complex is constructed from two apposed membranes, one usually enclosed within the other (Fig. 6, arrows). The striking and unique feature of this arrangement is that the two membranes are separated by a space of constant width. In transverse views of these paired membranes, the unit membrane of each of the two partners is clearly seen (Fig. 7), and the center-to-center distance between the two electron-lucent bilayers is ~ 15 nm.

FIGURE 2 Several views that show membrane having different degrees of crystallization of the ($\text{Na}^+ + \text{K}^+$)-ATPase molecules. These micrographs were obtained from membrane fragments of purified ($\text{Na}^+ + \text{K}^+$)-ATPase that had all been suspended in the same crystallization solution before the negative staining. A circular-shaped fragment of membrane having a region in which the surface particles have become clustered is shown in *A*, and a fragment of membrane containing several small patches that are formed from surface particles arranged in a crystalline mosaic, in *B*. A membrane where the surface particles have formed more extensive crystalline arrays is displayed in *C*. The region inside the rectangle displayed has a diffraction pattern such as the one shown in Fig. 3*B*. A large membrane fragment containing a high density of particles is presented in *D*. The curved arrows in *E*–*G* and the open arrow in *F* highlight membranes in which the surface particles form small clusters. The small arrowheads indicate regions where the particles form elongate, double rows of particles. Three regions (*H*), enclosed in the rectangles, contain rows of particles forming small arrays. These regions have diffraction patterns similar to the one in Fig. 4*B*. $\times 160,000$.

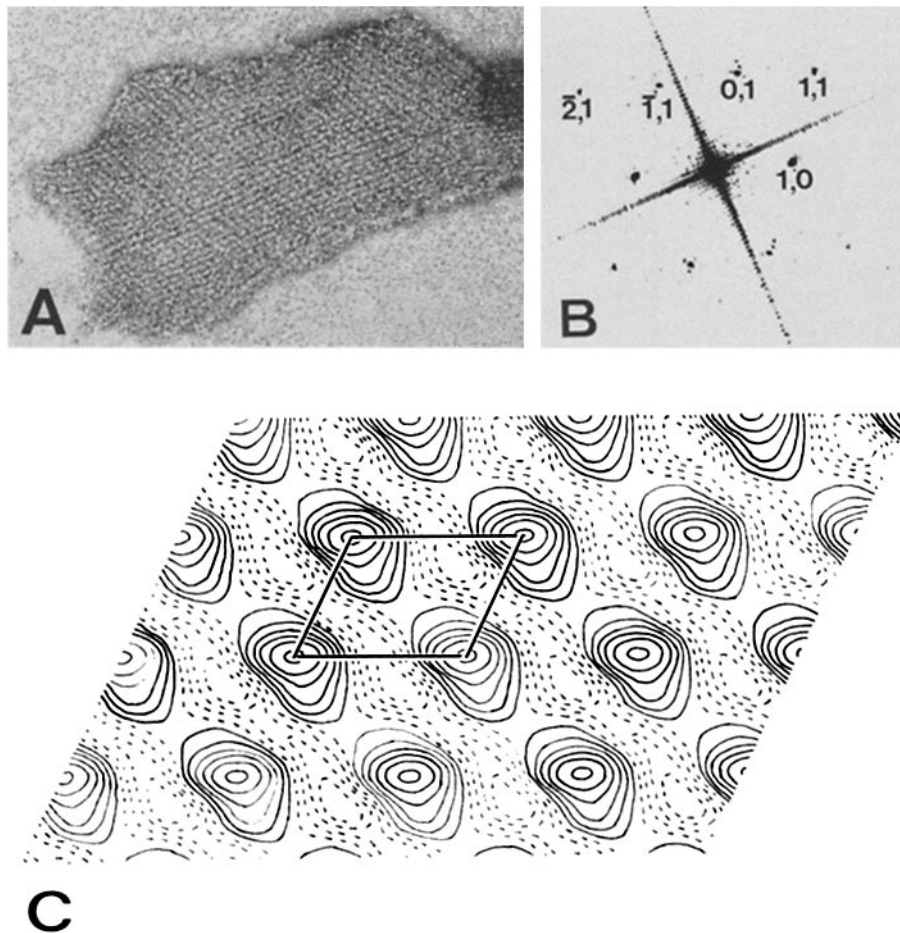


FIGURE 3 A fragment of membrane displaying the protomeric lattice of $(\text{Na}^+ + \text{K}^+)\text{-ATPase}$ molecules is shown in *A*. $\times 200,000$. The optical transform (*B*) of the array shows discrete reflections that indexed on a skew lattice. The lattice parameters of the array are $a = 6.0 \text{ nm}^{-1}$ and $b = 5.0 \text{ nm}^{-1}$. The membrane in *A* was also studied by Fourier methods (2). Arrays of optical densities were generated by scanning the negative with a microdensitometer at $25\text{-}\mu\text{m}$ intervals. Peak amplitudes and phases were obtained from the outputs of the computer for each one of the diffraction spots and then refined onto a common origin. The projection map in *C* was calculated by reverse Fourier transformation without imposing symmetry to the Fourier terms. The continuous lines correspond to the electron-lucent regions in the array (*A*), and therefore are the parts of the enzyme molecules exposed on the membrane surfaces. The broken lines correspond to the areas containing the negative stain.

The entire width of the structure, enclosing all electron-dense portions, is 23–25 nm.

Two observations support the conclusion that these novel complexes of paired membranes are constructed from $(\text{Na}^+ + \text{K}^+)\text{-ATPase}$. The first is that at least 90% of the protein was $(\text{Na}^+ + \text{K}^+)\text{-ATPase}$. The second was obtained through another experiment performed to establish this point. Microsomes at 2.0 mg ml^{-1} were treated with increasing amounts of SDS (0.0; 0.4; 0.5; 0.6; 0.65; and 0.7 mg ml^{-1}), and the membranes from each of these extractions were collected by centrifugation at the interface between 37.3% and 28.8% sucrose. Polyacrylamide gels of these fractions demonstrated that the proportion of the total protein that was $(\text{Na}^+ + \text{K}^+)\text{-ATPase}$ increased as the concentration of SDS used to extract the microsomal fraction was increased. Membranes from each of these samples were then suspended in crystallization medium, and the pellets were examined by thin sectioning. The frequency with which the paired membrane complexes were observed also increased as the concentration of SDS increased. Paired membrane complexes were observed, albeit at very low frequency, in crude microsomes that were not exposed to SDS. This observation rules out the possibility that the paired structures are the result of modifications on the enzyme caused by the detergent.

Several observations support the conclusion that the paired membranes are formed by the interaction of two previously independent membrane fragments containing crystalline arrays of the enzyme molecules. One is that these structures only occurred (Figs. 5 and 6) in preparations made from

membranes that had been exposed to the medium required to induce $(\text{Na}^+ + \text{K}^+)\text{-ATPase}$ to crystallize. The other is that the overall width of the complex is constant (Fig. 7) and the space separating both partners contains electron-dense septa connecting both plasma membranes (Fig. 7). The method of Sealock (36), which produces a layer of electron-dense material that embeds membranes and gives a negative contrast to the thin section, was used to confirm the crystalline nature of the paired membranes. Transverse, oblique, and “en face” views of the paired membranes prepared in this way are shown in Fig. 8. The paired membranes located in the center of Fig. 8*A*, as well as the one in Fig. 8*D*, have their gaps occupied by densely staining material outlining clear bands that repeat $\sim 7 \text{ nm}$ apart. Another view of the gap between the two partners shows two rows of particles running colinearly on either side of the middle line. This feature can be observed in the paired membranes at the right lower corner of Fig. 8*A* and in the Fig. 8*B*. There are also repeating deposits of electron-dense material located on the external surfaces of the paired membranes spaced $\sim 6\text{--}7 \text{ nm}$ apart. Oblique and “en face” views (Fig. 8, *C* and *E*) show that the planes of the membranes are occupied by particles that are spaced 7–8 nm apart.

When examined by negative staining, the paired membranes (Fig. 9) can be distinguished from single crystalline membranes (Fig. 3) by the thick roll seen around the edges of the structure where the membrane folds back upon itself. Views through such paired membranes (Fig. 9, *A* and *B*) display particles arranged in rows intersecting at angles that

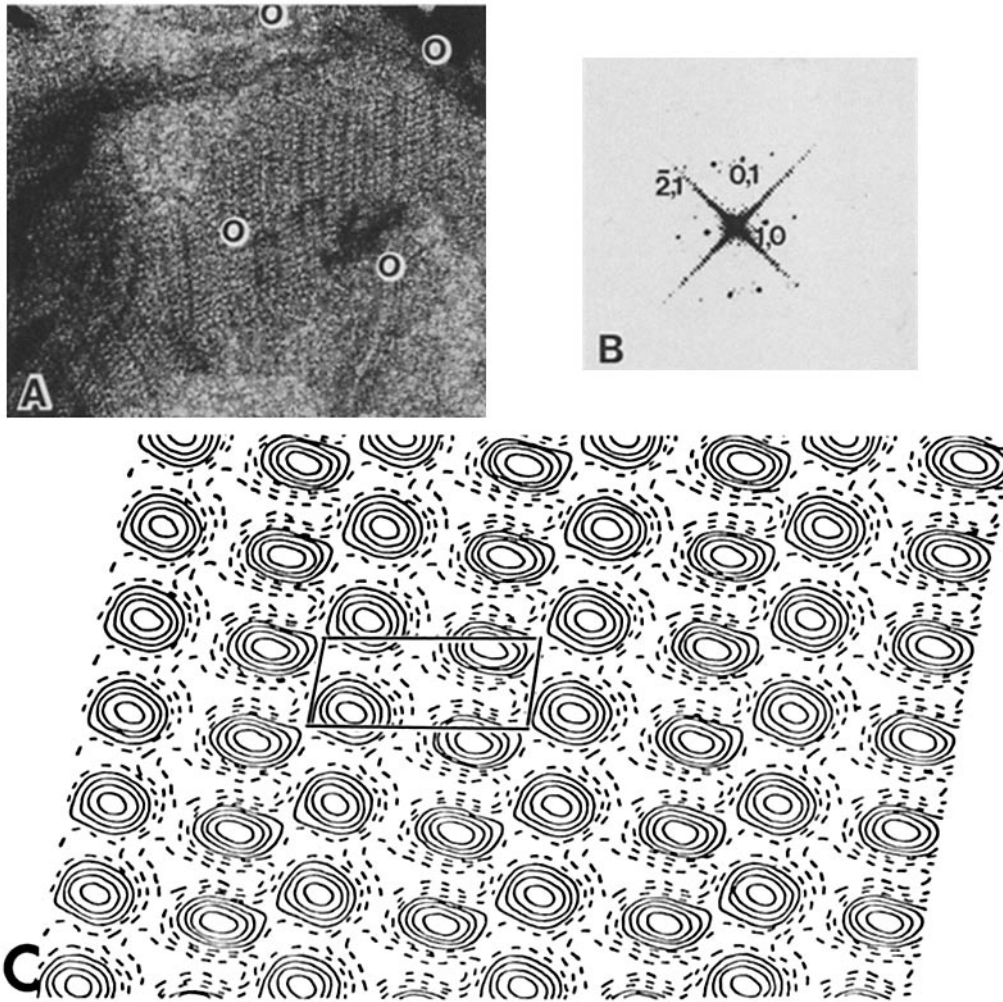


FIGURE 4 A shows a fragment of membrane with the diprotomeric array of the enzyme molecules that was studied by Fourier methods (region inside the zeros), $\times 200,000$. The optical transform (B) shows discrete reflections with lattice parameters $a = 12.5 \text{ nm}^{-1}$ and $b = 5.5 \text{ nm}^{-1}$. The projection map (C) was calculated by Fourier methods. Peak amplitudes and phases obtained for each diffraction spot were refined onto a common origin. The continuous lines in the projection map arise from the portion of the molecules surrounded by the stain.

are similar to those measured in the protomeric arrays found in single membranes. This observation suggests that adjacent $(\text{Na}^+ + \text{K}^+)\text{-ATPase}$ molecules from each of the apposed lattices forming the paired structure align colinearly.

Decoration of $(\text{Na}^+ + \text{K}^+)\text{-ATPase}$ with Agglutinin from *Ricinus communis*

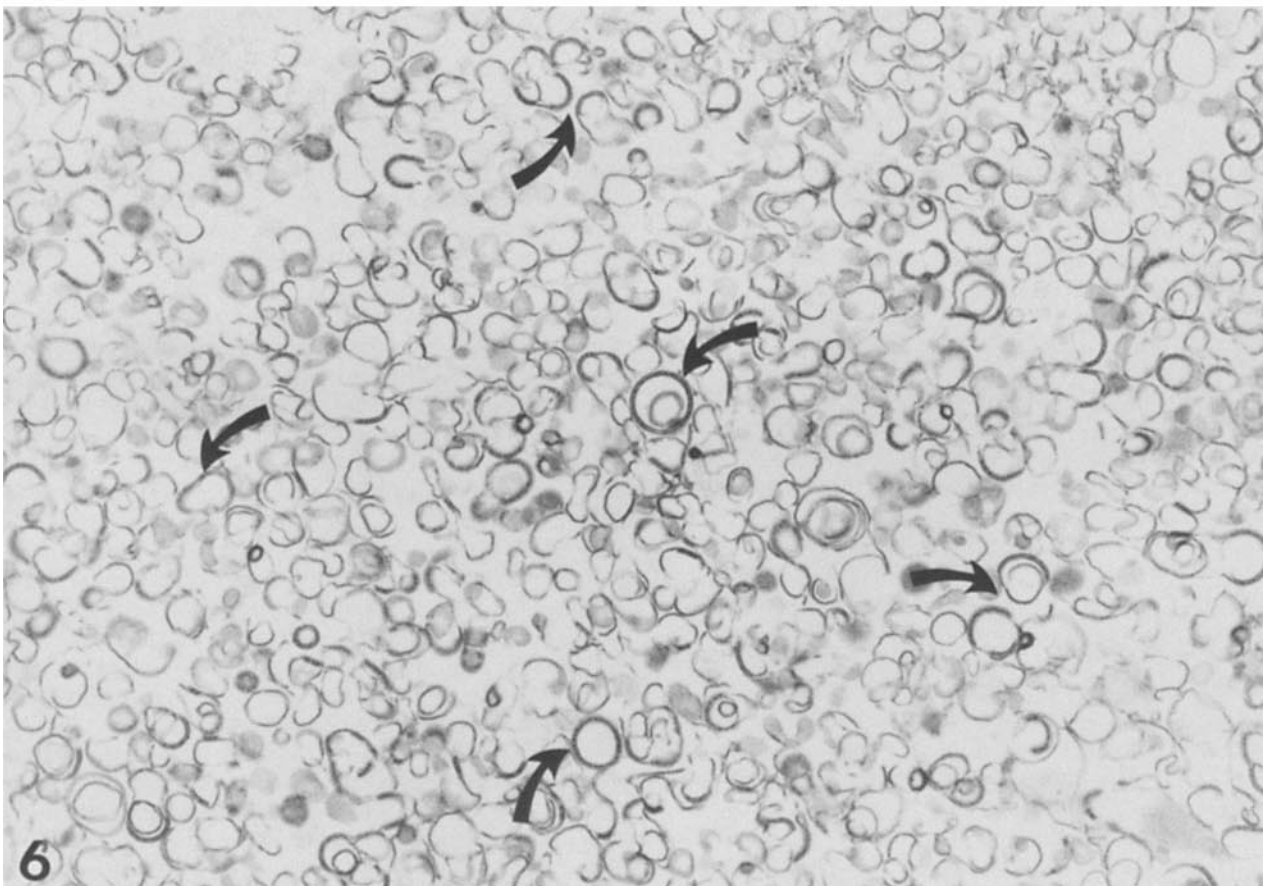
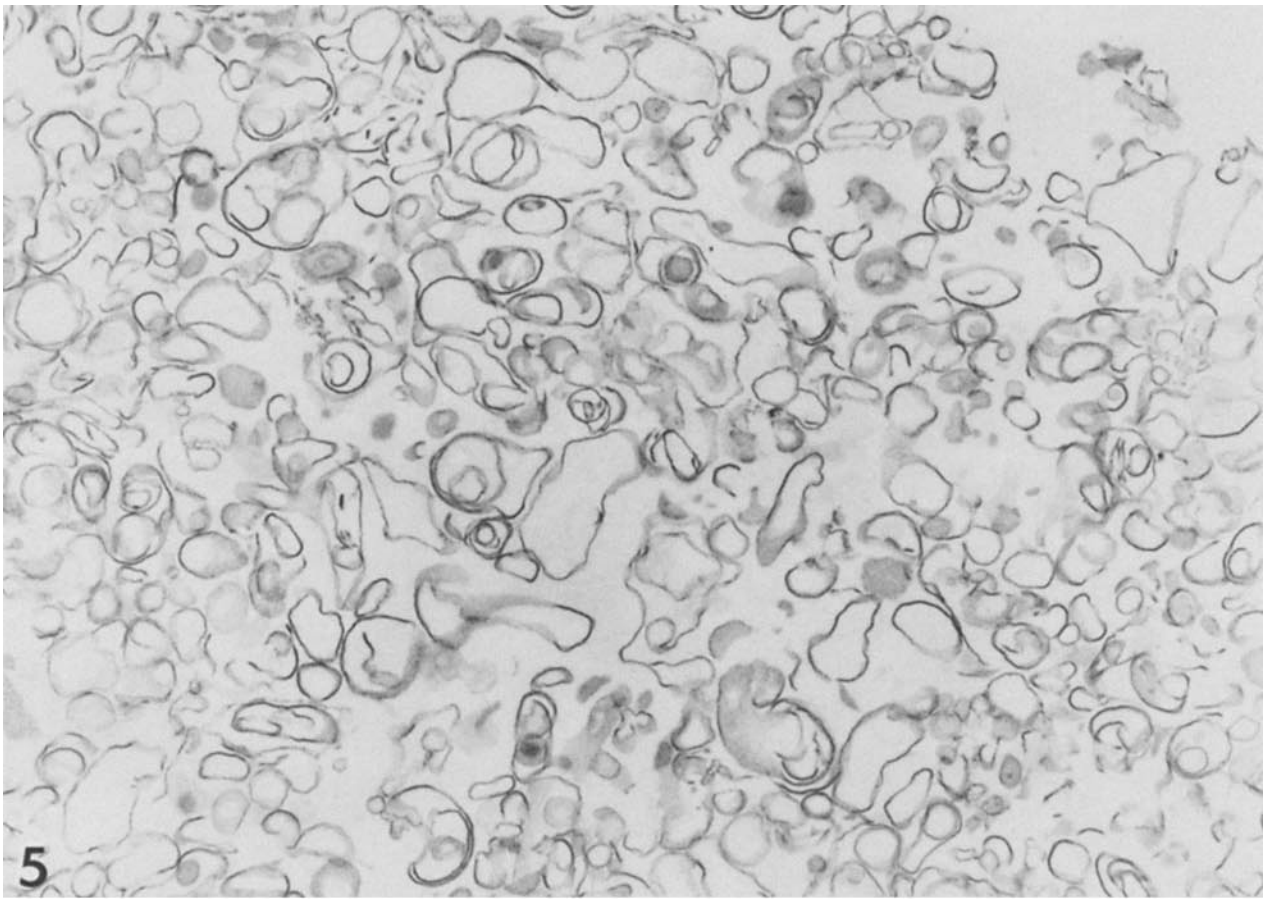
Additional evidence supporting the conclusion that the paired membranes are formed from $(\text{Na}^+ + \text{K}^+)\text{-ATPase}$ was obtained by decorating them with the agglutinin from *Ricinus communis*. This lectin is a sizable tetrameric protein of molecular weight 150,000, hence a minimum spherical diameter of 7.0 nm (31). It is also divalent and readily precipitates purified canine renal $(\text{Na}^+ + \text{K}^+)\text{-ATPase}$ quantitatively.⁴ Several paired membranes decorated with *Ricinus* agglutinin and visualized by the method of Sealock (39) are shown in Fig. 10. In heavily stained regions (arrows in Fig. 10, A and B), an additional electron-lucent layer parallel to one or both of the paired membranes and on the external surfaces of the doublet can be clearly observed. Since these layers were not detected in the controls on membranes that were not incubated with the agglutinin (Fig. 8), we have interpreted them as layers of agglutinin molecules each bound to polysaccharides on the β subunit of $(\text{Na}^+ + \text{K}^+)\text{-ATPase}$. Further features that support this interpretation are that the layer is approxi-

mately the predicted width ($\sim 5 \text{ nm}$), that it runs rigidly parallel to the adjacent membrane, and that it can be seen to run continuously into the regions where two of the paired membranes become joined through agglutinin molecules (Fig. 10, D and E). The distance between the center of the proximal bilayer of the paired membrane to the center of the layer of the agglutinin is 6.5–7 nm, while the distance between the centers of the two bilayers in the paired membranes is 15 nm, the same as that seen in the controls (Fig. 8) and in positively stained thin sections (Fig. 7).

Most importantly, the disposition of this layer of agglutinin molecules in the paired membrane complex also defines the orientation of the membranes in this duet. It can be deduced that the association that forms the pair is either the result of two extracytoplasmic or two cytoplasmic surfaces joining together. If the association were between an extracytoplasmic and a cytoplasmic surface, multilayers should have resulted, but we have not observed such structures. Thus the attachment of agglutinin to the outer surface of either paired membrane establishes that both are joined through the interaction of their cytoplasmic surfaces. Although the layers of agglutinin were often seen clearly on only one member of the paired membranes, there are many cases where both membranes are decorated (Fig. 10 C, F, and G).

Because the agglutinin is divalent, it can form a novel association between the paired membranes not seen in the controls (Fig. 8). For example, paired membranes can be joined together by a layer of agglutinin to form quartets, (Fig.

⁴ J. Kyte, unpublished observation.



FIGURES 5 and 6 Fig. 5: Representative view from a thin section obtained from a pellet of membrane-bound $(\text{Na}^+ + \text{K}^+)\text{-ATPase}$ bathed in the storage solution (0.25 M sucrose, 1 mM Na_2EDTA , 0.1% 2-mercaptoethanol, and 30 mM histidinium chloride). $\times 50,000$. Fig. 6: Representative view from a thin section obtained from a pellet of membrane-bound $(\text{Na}^+ + \text{K}^+)\text{-ATPase}$ bathed in crystallization medium. The arrows indicate some of the numerous, curved complexes of membrane formed by two apposed plasma membranes. $\times 50,000$.

10, *D* and *E*) or two plasma membranes can be bound together by a layer of the agglutinin (Fig. 10*H*). The quartets are particularly useful for measuring the precise dimensions of two regions (*X* and *Y* in Fig. 7, *D* and *E*) in the paired membranes. The one labeled *X*, the center-to-center distance between the bilayers of the two partners forming the paired membranes, is ~ 15 nm wide. The one labeled *Y*, the center-to-center distance between bilayers from adjacent paired membranes, is 17.5 nm wide. The former region is formed from the apposition of two cytoplasmic surfaces; the latter, from the apposition of two extracytoplasmic surfaces and a layer of agglutinin.

DISCUSSION

Crystalline arrays were produced in membranes of highly purified ($\text{Na}^+ + \text{K}^+$)-ATPase by manipulating the ionic conditions of the solution in which they were suspended. For several reasons it can be concluded that these arrays are formed from molecules of the enzyme. First, polyacrylamide gels (Fig. 1) of the fractions used for crystallization showed that 90% of the protein was accounted for by the α and β polypeptides of ($\text{Na}^+ + \text{K}^+$)-ATPase and that contaminants were only minor components. Second, the particles that form the crystalline arrays are indistinguishable from the particles on all of the noncrystalline membranes (Fig. 2), and, therefore, the former presumably are only a subpopulation of the large majority of the membrane-bound molecules of protein present in the sample. Third, the frequency with which the crystalline membrane-pairs appeared increased with the purity of the enzyme used for crystallization. Fourth, both the paired crystalline membranes were decorated by the agglutinin from *Ricinus communis*, a lectin that presumably binds to the polysaccharide moiety of the β subunit.

An entirely new structure was discovered when thin sections of the crystalline membranes were examined (Fig. 6). These were paired membranes (Figs. 7 and 8) that formed from two plasma membranes, each of which was composed of a crystalline array of ($\text{Na}^+ + \text{K}^+$)-ATPase and which adhered to each other as a result of an equally regular set of protein-protein interactions between their two respective cytoplasmic surfaces. The pattern in which these structures were decorated by the agglutinin of *Ricinus communis* (Fig. 10) shows that they formed through the interaction of the cytoplasmic surfaces of unilamellar membranes. Furthermore, the fact that, upon negative staining, the paired membranes have a projection (Fig. 9) similar to that of the protomeric crystals in unilamellar membranes (Fig. 2, *B* and *C*) leads to the conclusion that the molecules of enzyme opposite each other in the paired membranes lie colinearly atop each other. That such an arrangement is possible can be shown by superimposing (Fig. 9, *C-E*) two of the density maps of the monomeric array (Fig. 3) head-to-head. Such a structure allowed us to estimate two as yet unreported features of the membrane-bound enzyme. One is the total length of a molecule of ($\text{Na}^+ + \text{K}^+$)-ATPase along the axis normal to the membrane, and the other is the lengths of the extensions of the protein into the cytoplasmic and extracytoplasmic compartments.

The width of the region labeled *Y* in Fig. 10, *D* and *E* is the distance between the centers of two bilayers from adjacent paired membranes. This distance (*Y*) was found to be 17.5 nm. The diameter of the agglutinin is at least 7.0 nm, (*A*). If it is assumed that the space between adjacent bilayers in the

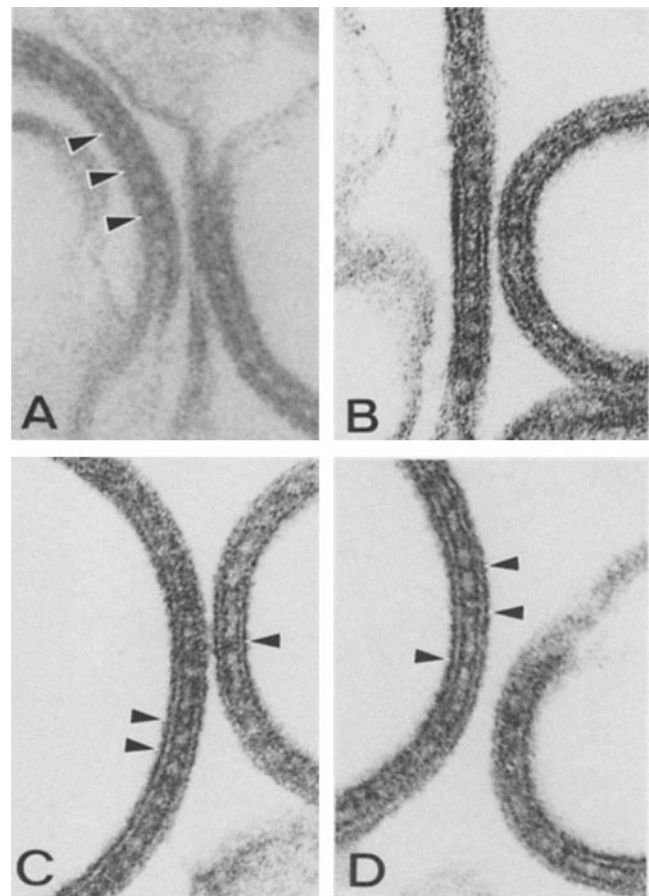


FIGURE 7 Gallery of selected transverse sections of paired membranes formed by bathing the enzyme in crystallization medium. The views were obtained from micrographs taken from three different experiments to demonstrate the reproducibility of the features of this unique complex. Each complex is formed by two unit membranes that are separated by a gap of constant width. The arrowheads in *A*, *C*, and *D* indicate electron-dense septa connecting the two plasma membranes. $\times 200,000$.

quartet is filled with two layers of the extracytoplasmic domains of ($\text{Na}^+ + \text{K}^+$)-ATPase sandwiching a layer of agglutinin molecules, then the distance from the center of the bilayer to the outer edge of the extracytoplasmic domain of ($\text{Na}^+ + \text{K}^+$)-ATPase would be 5.2 nm, $[(Y - A)/2]$. Alternatively, the distance from the center of the bilayer to the center of the layer of agglutinin in a decorated duet (Fig. 10, *A* and *B*) is 6.5–7 nm. Subtracting the radius of an agglutinin (3.5 nm) gives 3.5–4 nm for the distance from the center of the bilayer to the outer edge of the extracytoplasmic domain of ($\text{Na}^+ + \text{K}^+$)-ATPase. Convincing arguments could be made for the primacy of either of these estimates, so the best value for this dimension at this time is probably 3.5 nm. The center-to-center distance between the two bilayers in a paired membrane is 15 nm, and, therefore, the distance from the center of the bilayer to the outer edge of the cytoplasmic domain is 7.5 nm. The total length of the molecule (*c*) is thus 10.5–12.5 nm. This estimate of the thickness of the molecule is significantly different from those published by others (7, 13) who assumed 9 nm and 18 nm, respectively.

It was also possible to obtain estimates of the lengths of the portions of the enzyme molecule that protrude beyond the cytoplasmic and extracytoplasmic surfaces of the bilayer. For

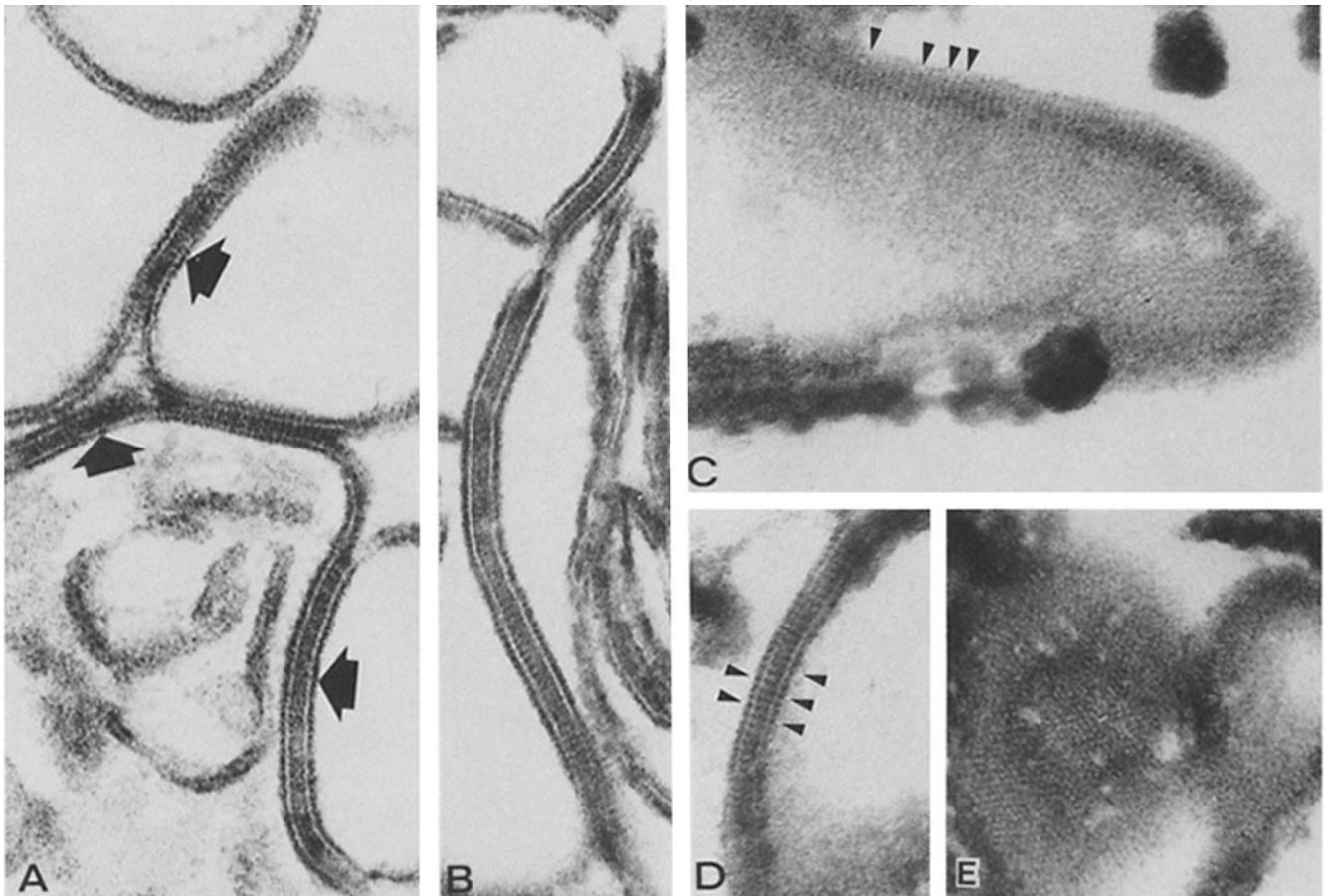


FIGURE 8 Selected views from thin sections of paired membranes produced by bathing the enzyme in crystallization medium and then fixing the pellets with tannic acid-glutaraldehyde (36). *A* shows that any given membrane can establish associations with several other isolated fragments (arrows, *A*). Note the set of densities located in the gap between the paired membranes in the center of *A*. *B* shows a transverse view displaying small particles located at each side of the boundary bisecting the complex. *C* is a tangential view of a complex of paired membranes. The rows of electron-lucent particles separated by electron-dense bands (arrowheads) suggest that existence of crystalline arrays in the gap between the two bilayers. *D* is a transverse view that displayed repetitive electron-dense septa (arrowheads) occupying the gap between the two membranes of the complex. Note that each electron-dense band in the gap coincides with an electron-dense spot on the free surface of the paired membranes. *E* is an en face view of the complex that demonstrates the presence of discrete particles in a crystalline array. $\times 200,000$.

that, we have assumed that the thickness of the bilayer, between the phosphorous atoms, is 4.8 nm. This thickness was obtained from measurements performed on phospholipid-cholesterol bilayers having a composition comparable to the one found in the crystalline membranes (25). With this value it can be calculated that the enzyme extends only 1–3 nm beyond the extracytoplasmic surface of the membrane but ~ 5 nm beyond the cytoplasmic surface. Therefore, the mass of the enzyme is asymmetrically distributed across the bilayer with a greater proportion on the cytoplasmic side than on the extracytoplasmic side. This observation is in agreement with previous studies indicating that at least the α subunit in the native enzyme has three to four times more surface area on the cytoplasmic side of the membrane than on the extracytoplasmic (30, 37).

Knowledge of the lattice parameters of the unit cell of $(\text{Na}^+ + \text{K}^+)\text{-ATPase}$ in the protomeric crystal allows the estimation of its volume ($a \times b \sin 65^\circ \times c = 320 \text{ nm}^3$). We can use this estimation to set an upper limit on the number of molecules

of $(\text{Na}^+ + \text{K}^+)\text{-ATPase}$ that could fit into this volume. The protein of one asymmetric unit, the $\alpha\beta$ protomer, should occupy $\sim 200 \text{ nm}^3$ (160,000 daltons at $1.23 \times 10^{-3} \text{ nm}^3 \text{ dalton}^{-1}$), and the volume of its carbohydrate moiety would be $\sim 8 \text{ nm}^3$ (7,800 daltons (23) at $1.06 \text{ nm}^3 \text{ dalton}^{-1}$). Although, in the noncrystalline membranes there are 140–150 nm^2 of lipid bilayer for every $\alpha\beta$ protomer, it is clear, that lipids must be excluded from the arrays during crystallization. All of these considerations demonstrate that each unit cell of the protomeric array contains one $\alpha\beta$ -protomer (7, 13, 40, 41). The diprotomeric array is formed from double rows of asymmetric units that are spaced in the a direction every 12.5 nm and in the b direction every 5.5 nm. If we assume the same thickness for this type of packing and use the same ingredients to fill this unit cell as those used previously for the protomeric array, it follows that this unit cell can accommodate two protomers.

Although our results are in close agreement with most of the observations presented in the literature (7, 13, 40, 41)—

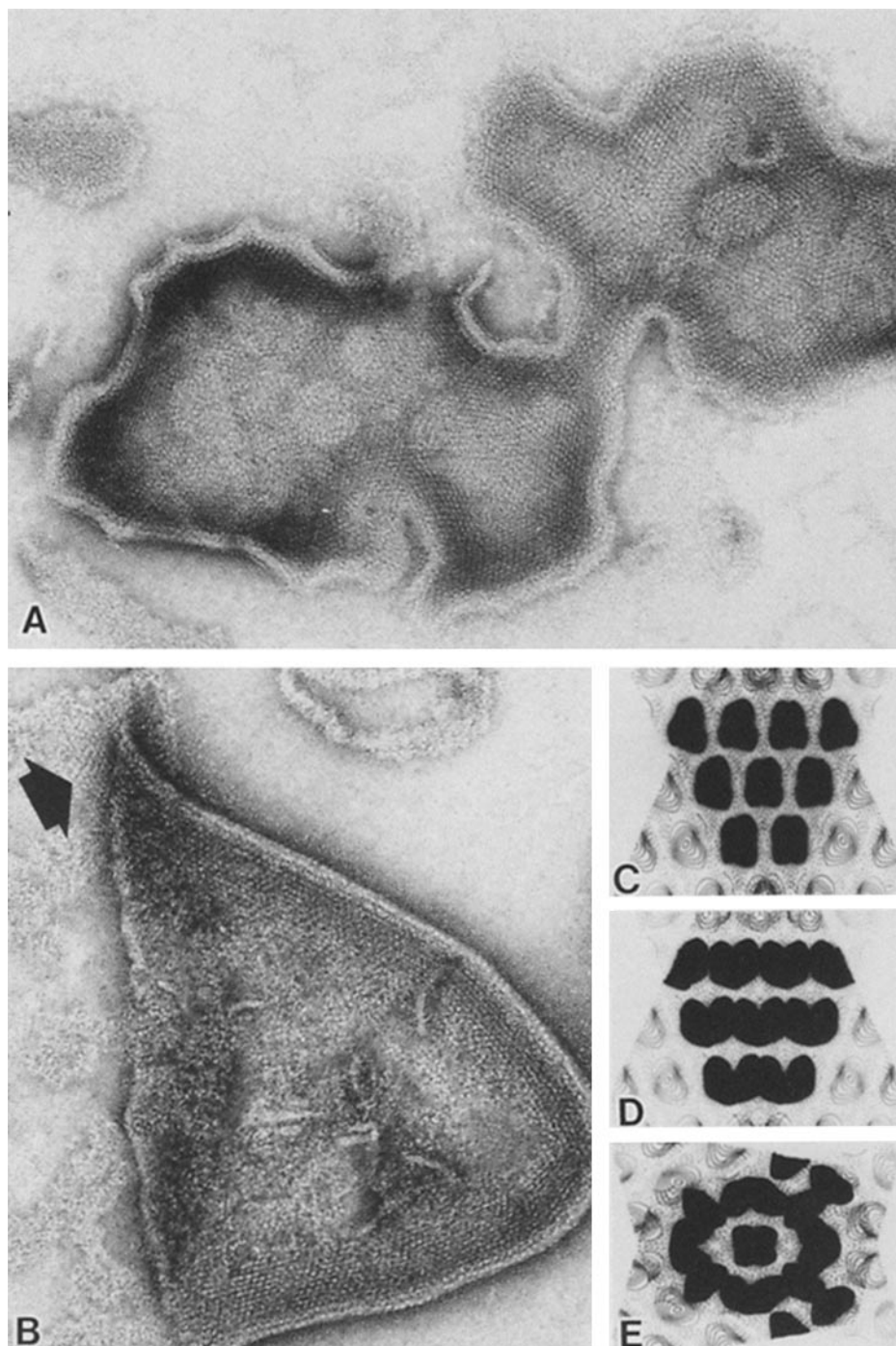
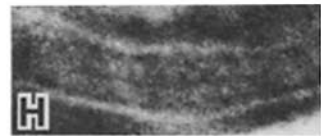
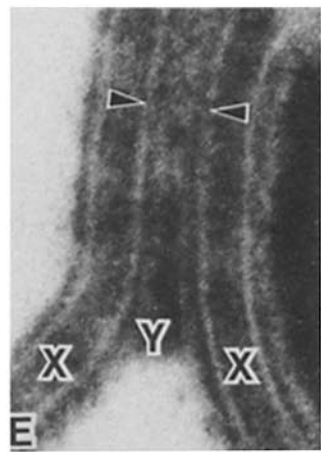
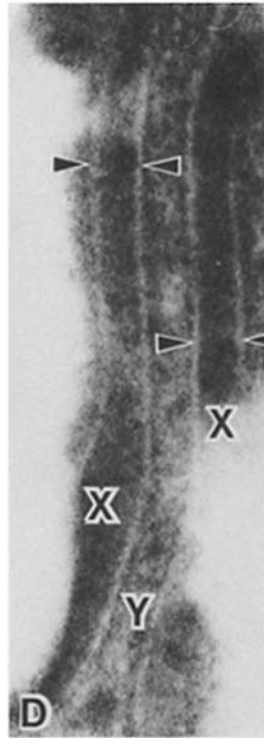
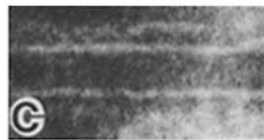
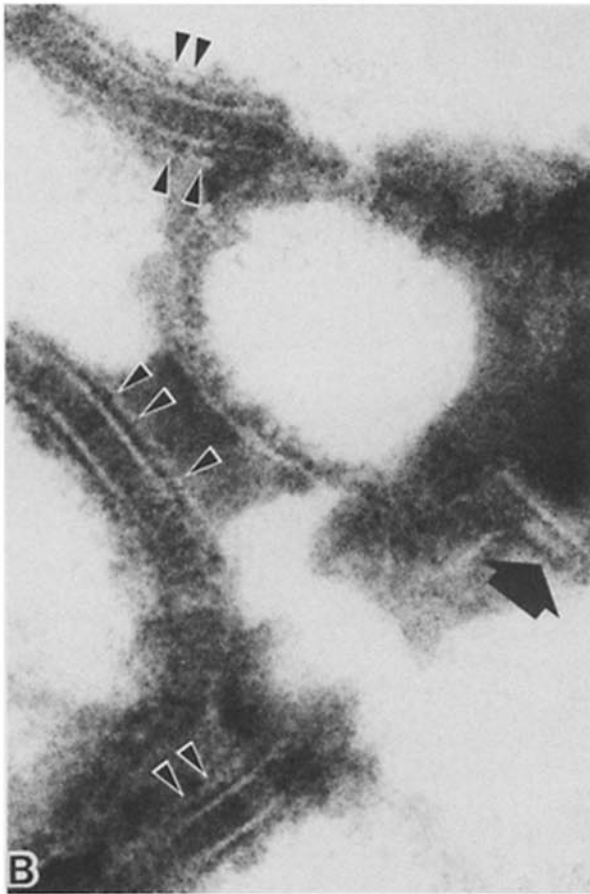
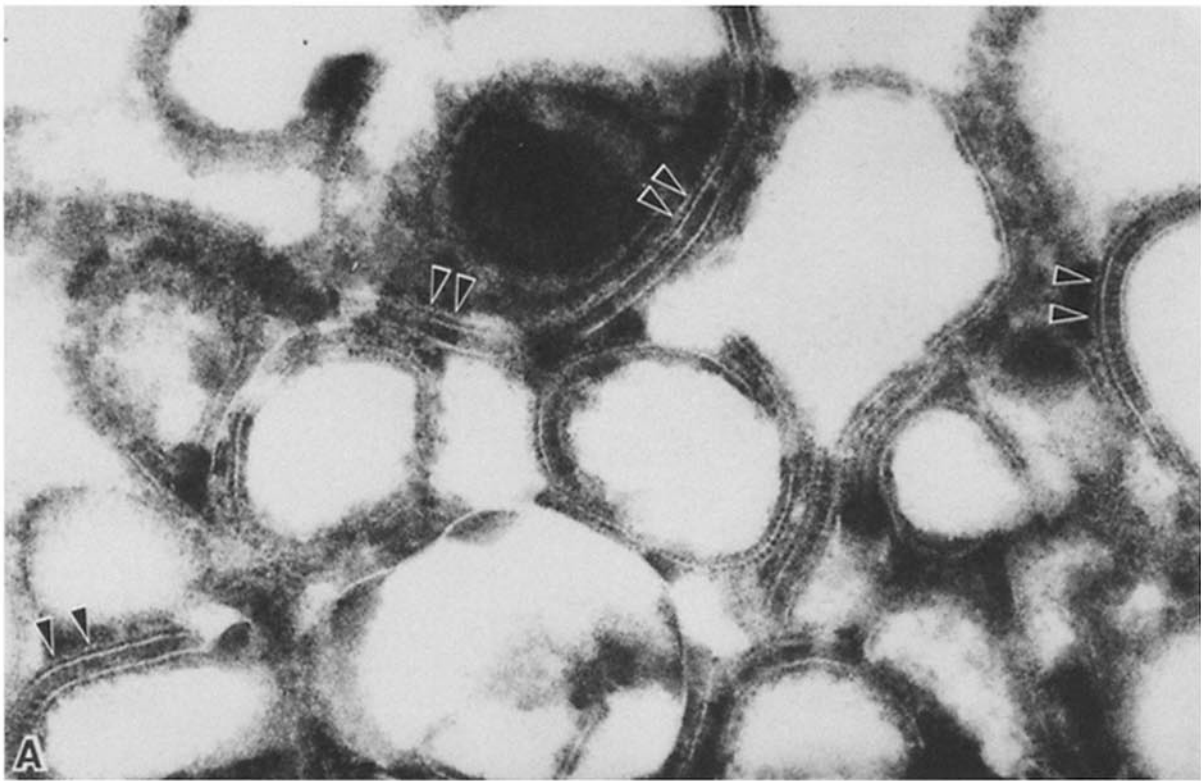


FIGURE 9 Negatively stained appearance of paired membranes. Note that the edges of these membranes are thicker and tend to accumulate larger amounts of stain. The membranes' surfaces show clearly distinguishable particles that are arranged in intersecting rows. The arrow in *B* indicates to a small piece of single membrane containing the lattice. $\times 200,000$. The bottom part of this figure shows a study in which the computer-calculated projection for the monomeric form of the enzyme (Fig. 3C) was drawn on transparent sheets, two of those sheets were superimposed head-to-head, and the regions of coincidence were blackened. The case when the monomers from the sheets were superimposed precisely one on top of the other is shown in *C*. A translation of one of the sheets along the *a* axis of the crystal was performed in *D*; and rotation of one of the sheets with respect to the other, in *E*. $\times 200,000$.

in particular, they confirm the recent reports of Skriver et al. (38) and Herbert et al. (16) regarding the packing arrangements adopted by the $(\text{Na}^+ + \text{K}^+)\text{-ATPase}$ molecules—several new and previously unreported observations have been made here. We have discovered conditions that lead to crystallization in a much shorter time and without the substantial loss of enzymatic activity encountered in the protocols using long incubations. We have demonstrated that the individual membranes form centrosymmetric structures, the paired membranes, when bathed in solutions leading to the formation of crystalline arrays. The presence of these centrosymmetric structures could simplify the calculation of one-dimensional

electron density profiles by low angle x-ray diffraction. Also, we have determined that these centrosymmetric structures arise from the interaction of the cytoplasmic surfaces of the membranes. From that information, we have estimated the overall length of a molecule of $(\text{Na}^+ + \text{K}^+)\text{-ATPase}$ and that it is asymmetrically located in the membrane.

We also found that two distinct crystalline arrays, protomeric and diprotomeric, would form under the same ionic conditions in the same specimen. Although this was an unexpected result, there is no reason to assume that this phenomenon has any special physiological significance. Similar behavior has been observed during the crystallization of sev-



eral soluble proteins. For example, the crystal forms IIA and IIB of glutamine synthetase grow intermingled from the same solution (15). Also, in the case of membrane proteins, the crystals formed by the same protein are often different when conditions unrelated to their functions are altered. For example, the purple membrane protein of the *H. halobium* exists in a hexagonal lattice in the native bacterium, but it is orthorhombic when recrystallized *in vitro* (27). Another well-known example is cytochrome oxidase, which adopts different plane group symmetry depending on the detergent used in the preparation of the crystalline specimens (12).

Although a complete three-dimensional determination of the structure of $(\text{Na}^+ + \text{K}^+)\text{-ATPase}$ in its membrane-bound form is the next step, the different observations gathered in this study provide important preliminary information regarding the size, overall shape, and its asymmetric location of the molecule within the membrane.

We wish to thank Dr. P. N. T. Unwin for advice and for helpful discussions as well as the use of his automatic microdensitometer. Also, we wish to thank Dr. D. Grano and Dr. L. A. Amos for computer programs used in the image-processing section, and James Gallagher for preparing the various samples of $(\text{Na}^+ + \text{K}^+)\text{-ATPase}$ used in these studies.

This research was supported in part by the MDA Jerry Lewis Neuromuscular Research Center Grant, to G. Z., and grant AM-07233 from the National Institutes of Health; Grant PCM 81-18108 from the National Science Foundation; and Grant-in-Aid AHA 81-1003 from the American Heart Association, to J. K.

Received for publication 26 May 1983, and in revised form 5 January 1984.

REFERENCES

- Ames, B. N., and D. T. Dubin. 1960. The role of polyamines in the neutralization of bacteriophage deoxyribonucleic acid. *J. Biol. Chem.* 235:769-775.
- Amos, L. A., R. Henderson, and P. N. T. Unwin. 1982. Three-dimensional structure determination by electron microscopy of two-dimensional crystals. *Prog. Biophys. Mol. Biol.* 39:183-231.
- Brotherus, J. R., J. V. Møller, and P. L. Jørgensen. 1981. Soluble and active renal $\text{Na}_2\text{K-ATPase}$ with maximum protein molecular weight $170,000 \times 9,000$ daltons; formation of larger units by secondary aggregation. *Biochem. Biophys. Res. Commun.* 100:146-154.
- Craig, W. S., and J. Kyte. 1980. Stoichiometry and molecular weight of the minimum asymmetric unit of canine renal sodium and potassium ion-activated adenosine triphosphatase. *J. Biol. Chem.* 255:6262-6269.
- Craig, W. S. 1982. Determination of the distribution of sodium and potassium activated adenosinetriphosphatase among the various oligomers formed in solutions of nonionic detergents. *Biochemistry.* 21:2667-2674.
- Craig, W. S. 1982. Monomer of sodium and potassium ion activated adenosine triphosphatase displays complete enzymatic function. *Biochemistry.* 21:5707-5717.
- Deguchi, N., P. L. Jørgensen, and A. B. Maunsbach. 1977. Ultrastructure of the sodium pump. Comparison of thin sectioning, negative staining, and freeze-fracture of purified, membrane-bound $(\text{Na}^+ + \text{K}^+)\text{-ATPase}$. *J. Cell Biol.* 75:619-634.
- Dixon, J. F., and L. E. Hokin. 1974. Studies on the characterization of the sodium-potassium transport adenosine triphosphatase. *Arch. Biochem. Biophys.* 163:749-758.
- Erickson, H. P., and A. Klug. 1971. Measurement and compensation of defocusing and aberrations by Fourier processing of electron micrographs. *Philos. Trans. R. Soc. Lond. B. Biol. Sci.* 261:105-118.

- Erickson, H., W. A. Voter, and K. Leonard. 1978. Image reconstitution in electron microscopy enhancement of periodic structure by optical filtering. *Methods Enzymol.* 49 (Pt. G):39-63.
- Esmann, M., C. Christiansen, K.-A. Karlsson, G. C. Hausson, and J. C. Skou. 1980. Hydrodynamic properties of solubilized $(\text{Na}^+ + \text{K}^+)\text{-ATPase}$ from rectal glands of *Squalus acanthias*. *Biochim. Biophys.* 603:1-12.
- Fuller, S. D., R. A. Capaldi, and R. Henderson. 1979. Structure of cytochrome *c* oxidase in deoxycholate-derived two-dimensional crystals. *J. Mol. Biol.* 134:305-327.
- Haase, J. W., and H. Koepsell. 1979. Substructure of membrane-bound $(\text{Na}^+ + \text{K}^+)\text{-ATPase}$ protein. *Pflügers Arch.* 381:127-135.
- Hasting, D. F., and J. A. Reynolds. 1979. Molecular weight of $(\text{Na}^+ + \text{K}^+)\text{-ATPase}$ from shark rectal gland. *Biochemistry.* 18:817-821.
- Heidner, E. G., T. G. Frey, J. Held, L. J. Weissman, R. E. Fenna, M. Lei, M. Hare, H. Kabsch, R. M. Sweet, and D. Eisenberg. 1978. New crystal forms of glutamine synthetase and implications for the molecular structure. *J. Mol. Biol.* 122:163-173.
- Herbert, H., P. L. Jørgensen, E. Skriver, and A. B. Maunsbach. 1982. Crystallization patterns of membrane-bound $(\text{Na}^+ + \text{K}^+)\text{-ATPase}$. *Biochim. Biophys. Acta.* 689:571-574.
- Hermann, R., R. Jaenicke, and R. Rudolf. 1981. Analysis of the reconstitution of oligomeric enzymes by cross-linking with glutaraldehyde: kinetics of reassociation of lactic dehydrogenase. *Biochemistry.* 20:5195-5201.
- Hokin, L. E., J. L. Dahl, J. D. Deupree, J. F. Dixon, J. F. Hackney, and J. F. Perdue. 1973. Studies on the characterization of the sodium-potassium transport adenosine triphosphatase. *J. Biol. Chem.* 248:2593-2605.
- Jørgensen, P. L., and J. C. Skou. 1969. Preparation of highly active $(\text{Na}^+ + \text{K}^+)\text{-ATPase}$ from other medulla of rabbit kidney. *Biochem. Biophys. Res. Commun.* 37:39-46.
- Jørgensen, P. L. 1974. Purification and characterization of $(\text{Na}^+ + \text{K}^+)\text{-ATPase}$. III. Purification from the outer medulla of mammalian kidney after selective removal of membrane components by sodium dodecylsulphate. *Biochem. Biophys. Acta.* 356:36-52.
- Kyte, J. 1971. Purification of the sodium- and potassium-dependent adenosine triphosphatase from canine renal medulla. *J. Biol. Chem.* 246:4157-4165.
- Kyte, J. 1972. Properties of the two polypeptides of sodium- and potassium-dependent adenosine triphosphatase. *J. Biol. Chem.* 247:7642-7649.
- Kyte, J. 1975. Structural studies of sodium and potassium ion-activated adenosine triphosphatase. *J. Biol. Chem.* 250:7443-7449.
- Kyte, J. 1981. Molecular considerations relevant to the mechanism of active transport. *Nature (Lond.)* 292:201-204.
- Lecuyer, H., and D. G. Dervichian. 1969. Structure of aqueous mixtures of lecithin and cholesterol. *J. Mol. Biol.* 45:39-57.
- Liang, S. M., and C. G. Winter. 1977. Digitonin-induced changes in subunit arrangement in relation to some *in vitro* activities of the $(\text{Na}^+ + \text{K}^+)\text{-ATPase}$. *J. Biol. Chem.* 252:8278-8284.
- Michel, H., D. Oesterhelt, and R. Henderson. 1980. Orthorhombic two-dimensional crystal form of purple membrane. *Proc. Natl. Acad. Sci. USA.* 77:338-342.
- Moczydlowski, E. G., and P. A. G. Fortes. 1981. Inhibition of sodium and potassium adenosine triphosphatase by 2', 3'-O-(2,4,6-trinitrocyclohexadienylidene) adenine nucleotides. *J. Biol. Chem.* 256:2357-2366.
- Munson, K. B. 1981. Light-dependent inactivation of $(\text{Na}^+ + \text{K}^+)\text{-ATPase}$ with a new photoaffinity reagent, chromium arylazido- β -alaninyl ATP. *J. Biol. Chem.* 256:3223-3230.
- O'Connell, M. A. 1982. Exclusive labeling of the extracytoplasmic surface of sodium and potassium ion-activated adenosine triphosphatase and a determination of the distribution of surface area across the bilayer. *Biochemistry.* 21:5984-5991.
- Olsnes, S., E. Salvedt, and A. Pihl. 1974. Isolation and comparison of galactose-binding lectins from *Abrus precatoricus* and *Ricinus communis*. *J. Biol. Chem.* 249:803-810.
- Peterson, G. L., and L. E. Hokin. 1981. Molecular weight and stoichiometry of the sodium- and potassium-activated adenosine triphosphatase subunits. *J. Biol. Chem.* 256:3751-3761.
- Riva, A. 1974. A simple and rapid staining method for enhancing the contrast of tissues previously treated with uranyl acetate. *J. Microsc. (Paris)* 19:105-108.
- Ruoho, A., and J. Kyte. 1974. Photoaffinity labeling of the ouabain-binding site on $(\text{Na}^+ + \text{K}^+)\text{-adenosine triphosphatase}$. *Proc. Natl. Acad. Sci. USA.* 71:2352-2356.
- Salmon, E. D., and D. DeRosier. 1981. A surveying optical diffractometer. *J. Microsc. (Oxf.)* 123:239-247.
- Sealock, R. 1982. Cytoplasmic surface structure in postsynaptic membranes from electric tissue visualized by tannic-acid-mediated negative contrasting. *J. Cell Biol.* 92:514-522.
- Sharkey, R. G. 1983. Lactoperoxidase-catalyzed iodination of sodium and potassium ion-activated adenosinetriphosphatase in the Madin-Darby canine kidney epithelial cell line and canine renal membranes. *Biochim. Biophys. Acta.* 730:327-341.
- Skriver, E., A. B. Maunsbach, and P. L. Jørgensen. 1981. Formation of two-dimensional crystals in pure membrane-bound $\text{Na}^+ + \text{K}^+\text{-ATPase}$. *FEBS (Fed. Eur. Biochem. Soc.) Lett.* 131:219-222.
- Uesugi, S., N. C. Dulak, J. F. Dixon, T. D. Hexum, J. L. Dahl, J. F. Perdue, and L. E. Hokin. 1971. Studies on the characterization of the sodium-potassium transport adenosine triphosphatase. *J. Biol. Chem.* 246:531-543.
- Van Winkle, W. B., L. K. Lane, and A. Schwartz. 1976. The subunit fine structure of

FIGURE 10 Micrographs from thin sections of membrane-bound $(\text{Na}^+ + \text{K}^+)\text{-ATPase}$ bathed in crystallization medium and then decorated with the agglutinin from *Ricinus communis*. Pellets were prepared using the method described by Sealock (40) to allow a direct visualization of the lectin. A low-magnification view of a field that shows numerous paired membranes sectioned transversely is present in A. The triangles point out a new layer of electron-lucent material associated with the free surfaces of the paired membranes. Three short segments of paired membranes and a single membrane (arrow) decorated by the agglutinin (compare with undecorated controls in Fig. 8, A, B, and D) are shown in B. Sections of paired membranes where both free surfaces are decorated with layers of electron-lucent material that appeared as the result of the incubation with the agglutinin are shown in C, F, and G. Quartets, formed from the interaction of two adjacent double membranes through their layers of agglutinin, are seen in D and E. The dimensions labeled X correspond to the distance between the centers of the two bilayers forming each of the paired membranes. The dimension labeled Y corresponds to the space between two adjacent paired membranes formed by the surfaces that complexed the agglutinin. Two single membranes bound together by the agglutinin layers can be seen in H. $\times 160,000$ (A); $\times 360,000$ (B); $\times 400,000$ (C-H).

- isolated, purified $\text{Na}^+ + \text{K}^+$ -Adenosine Triphosphatase. Freeze-fracture study. *Exp. Cell Res.* 101:291-296.
41. Vogel, F., H. W. Meyer, R. Grosse, and H. R. H. Repke. 1977. Electron microscopic visualization of the arrangement of the two protein components of $(\text{Na}^+ + \text{K}^+)\text{-ATPase}$. *Biochim. Biophys. Acta.* 470:497-502.
42. Weber, K., and M. Osborn. 1969. The reliability of molecular weight determinations by dodecyl sulfate-polyacrylamide gel electrophoresis. *J. Biol. Chem.* 244:4406-4412.
43. Winslow, J. 1981. The reaction of sulfhydryl groups of sodium and potassium ion-activated adenosine triphosphatase with *N*-ethylmaleimide. *J. Biol. Chem.* 256:9522-9531.
44. Zampighi, G., J. W. Freytag, and J. Kyte. 1983. The structural organization of the isolated, membrane-bound $(\text{Na}^+ + \text{K}^+)\text{-ATPase}$. *Biophys. J.* 41:4a. (Abstr.)